Protein−Carbohydrate Interactions in Human Lysozyme Probed by Combining Site-Directed Mutagenesis and Affinity Labeling†

Michiro Muraki* and Kazuaki Harata

Biomolecules Department, National Institute of Bioscience and Human-Technology, 1-1 Higashi, Tsukuba, Ibaraki 305-8566, Japan

Naoki Sugita and Ken-ichi Sato

Faculty of Engineering, Kanagawa University, Yokohama, Kanagawa 221-0802, Japan

Received June 18, 1999; Revised Manuscript Received September 2, 1999

ABSTRACT: The synergism between apolar and polar interactions in the carbohydrate recognition by human lysozyme (HL) was probed by site-directed mutagenesis and affinity labeling. The three-dimensional structures of the Tyr63→Leu mutant HL labeled with 2′,3′-epoxypropyl β-glycoside of *N*,*N*′-diacetylchitobiose (L63-HL/NAG-NAG-EPO complex) and the Asp102→Glu mutant HL labeled with the 2′,3′-epoxypropyl β-glycoside of *N*-acetyllactosamine were revealed by X-ray diffraction at 2.23 and 1.96 Å resolution, respectively. Compared to the wild-type HL labeled with the 2′,3′-epoxypropyl β-glycoside of *N*,*N*′-diacetylchitobiose, the *N*-acetylglucosamine residue at subsite B of the L63-HL/NAG-NAG-EPO complex markedly moved away from the 63rd residue, with substantial loss of hydrogen-bonding interactions. Evidently, the stacking interaction with the aromatic side chain of Tyr63 is essential in positioning the *N*-acetylglucosamine residue in the productive binding mode. On the other hand, the position of the galactose residue in subsite B of HL is almost unchanged by the mutation of Asp102 to Glu. Most hydrogen bonds, including the one between the carboxylate group of Glu102 and the axial 4-OH group of the galactose residue, were maintained by local movement of the backbone from residues 102−104. In both structures, the conformation of the disaccharide was conserved, reflecting an intrinsic conformational rigidity of the disaccharides. The structural analysis suggested that CH−π interactions played an important role in the recognition of the carbohydrate residue at subsite B of HL.

A number of important biological phenomena, such as glycolysis, sugar transport, and immunological events, depend largely on protein−carbohydrate interactions (*1*, *2*). Human lysozyme (HL)[1] is an enzyme that shows hydrolyzing activity against bacterial cell walls or chitin (*3*, *4*), and recently it has been recognized as the anti-HIV component in the preparation of human chorionic gonadotropin (*5*). Carbohydrate-binding proteins have been classified into two major groups by their overall shape of the ligand-binding sites (*6*). The first group, to which HL belongs, has a buried, ligand-engulfing binding site, and the second group including lectin families possesses a shallow ligand-binding site. Despite this difference in the binding site morphology, the recognition processes found in all structurally characterized carbohydrate-binding proteins so far are governed by two major stereochemical principles (*6*−*9*). The first type of stereochemical forces relevant to recognition are the hydrogen-bonding interactions involving the hydroxyl groups of the carbohydrate moiety and the polar groups of protein, and the other important forces are the less polar van der Waals interaction involving the C-H group of the carbohydrate moiety and the aromatic side chains of protein molecules. In order to reveal the structural basis of carbohydrate recognition, quite a few three-dimensional structures of carbohydrate-binding proteins, including *c*-type lysozymes, complexed with their specific ligands, have been characterized in atomic detail (*10*−*15*). The study of the lectin-binding sites of legume revealed the determinants in the selection of mannose/glucose over galactose (*16*).

Both site-directed mutagenesis of a protein molecule and specific modification of a carbohydrate ligand should contribute significantly to our understanding of such interactions. Nevertheless, due to the synergism of hydrogen-bonding and van der Waals interactions in the protein−carbohydrate complex (*9*, *17*), a small structural alteration in either can make the interaction energetically unfavorable and completely alter the binding mode of the ligand. Actually, either the mutation of Trp62 (the corresponding residue in HL is Tyr63) to Gly or the replacement of Asp101 (Asp102 in HL) to Gly changed the binding mode of *N*,*N*′-diacetylchitobiose to nonproductive ones (*18*) in several mutant hen egg-white lysozyme/saccharide complexes reported by Maenaka et al. (*18*, *19*). Hence, the impact of the

† This work was supported by a grant from the Agency of Industrial Science and Technology, MITI, Japan.

* Author to whom correspondence should be addressed. Phone: 81 298-54-6193. Fax: 81 298-54-6194. E-mail address: muraki@nibh.go.jp.

[1] Abbreviations: HL, human lysozyme (1,4-β-*N*-acetylmuraminidase, EC 3.2.1.17); NAG-NAG-EPO, 2′,3′-epoxypropyl *O*-β-*N*-acetyl-D-glucosaminyl-(1→4)-β-*N*-acetylglucosamine; GAL-NAG-EPO, 2′,3′-epoxypropyl *O*-β-*N*-acetyl-D-galactopyranosyl-(1→4)-β-*N*-acetylglucosamine; rms, root-mean-square; MALDI-TOF/MS, matrix-assisted laser desorption ionization-time of flight mass spectrometry.

10.1021/bi991402q CCC: $19.00 © 2000 American Chemical Society
Published on Web 12/17/1999

mutation on the productive binding mode could not be assessed.

A promising solution to remedy this technical dilemma involves the combination of site-directed mutagenesis and affinity labeling. An irreversible saccharide inhibitor has been widely used to identify the active site residues of glycosidases (*20*, *21*). The use of the 2′,3′-epoxypropyl β-glycoside of *N*-acetylglucosamine oligomers was originally described by Thomas et al. (*22*), who reported irreversible inhibition of the lytic activity of hen egg-white lysozyme and the identification of Asp52 (Asp53 in HL) as the site of attachment of the label.

In previous work, we demonstrated that the protein−carbohydrate interaction mode in the wild-type HL labeled by NAG-NAG-EPO (*23*) was indistinguishable from that of free ligand/HL complex in the productive binding mode (*13*). Recently, we succeeded in characterizing the interactions between wild-type HL and disaccharides with weaker affinity compared to *N*,*N*′-diacetylchitobiose using this same technique (*23*−*25*). In this paper, we describe the first application of affinity labeling to site-directed mutants of HL, in an attempt to gain an improved understanding of protein−carbohydrate interactions in β1,4-linked saccharide-binding proteins.

MATERIALS AND METHODS

Preparation of the Affinity-Labeled Mutant HLs. The production and purification of mutant HLs were performed as described elsewhere (*26*). The sequences of oligonucleotide primers used for directed mutations, Asp102→Asn and Asp102→Glu, were CGTTAGAAACCCACAAGG and CGTTAGAGAACCACAAGG, respectively. The mismatched base from the original sequence (*27*) is underlined. The concentration of purified mutant HLs was determined by the BCA protein assay kit (Pierce), with wild-type HL used as the standard. Lyophilized *Micrococcus luteus* cells were purchased from Sigma. The apparent affinity constant against *M. luteus* cells and the maximal velocity of lytic action were determined according to the method of Locquet et al. (*28*). The lysis of *M. luteus* cells in 50 mM potassium phosphate (pH 6.2) was monitored at 650 nm. The concentration of *M. luteus* cells was varied over a 10-fold range (50−500 μg/mL), and the kinetic constant was evaluated from least-squares analysis of conventional double-reciprocal plots. The apparent binding constant, $K_{M,app}$, was expressed as micrograms of *M. luteus* cells per milliliter. The maximal velocity, V_{max}, was expressed as the absorbance change at 650 nm (A_{650}) per microgram of enzyme per minute.

The affinity labeling reagents were synthesized organochemically according to the method of Thomas (*29*), followed by NMR to verify purity (*23*). The reaction of mutant HLs with the affinity labeling reagents was performed by incubating either Leu63-mutant HL (5 mg) or Glu102-mutant HL (10 mg) with the affinity labeling reagent (25 mg) in 1.5 mL of 0.2 M sodium acetate buffer (pH 5.4). After 72 h incubation at 37 °C, the reaction mixture was separated by cation-exchange chromatography using MonoS HR5/5 (Pharmacia). The residual activity was then evaluated by the initial decrease of absorbance at 650 nm within 0.75 min. Molecular weights were determined by MALDI-TOF/MS analysis (Voyager, PerSeptive Biosystems) for peak fractions (Figure 1), which were pooled and dialyzed against 0.13 mM sodium acetate buffer (pH 4.5) at 4 °C. After dialysis, the samples were lyophilized and used in crystallization experiments.

Crystallization and Structure Determination. Crystallization of the affinity-labeled mutant HLs was performed as described (*23*). Diffraction data were collected on an Enraf-Nonius FAST diffractometer with a FR571 generator (40 kV, 60 mA). A software package, X-PLOR ver. 3.1 (*30*), was used to solve the structures by molecular replacement. The refined coordinates of the wild-type HL labeled with the 2′,3′-epoxypropyl β-glycoside of *N*,*N*′-diacetylchitobiose (WT-HL/NAG-NAG-EPO complex) [PDB code: 1REY (*23*)] with a modeled replacement of Tyr63 with Leu and that of the wild-type HL labeled with the 2′,3′-epoxypropyl β-glycoside of *N*-acetyllactosamine (WT-HL/GAL-NAG-EPO complex) [PDB code: 1REZ (*23*)] with a modeled replacement of Asp102 with Glu were used as search models. The number of protein molecules in the asymmetric unit was estimated to be 1 as judged by the V_m value [1.91 Å^3 Da^{-1} for the Leu63-mutant HL labeled with the 2′,3′-epoxypropyl β-glycoside of *N*,*N*′-diacetylchitobiose (L63-HL/NAG-NAG-EPO complex) and 1.90 Å^3 Da^{-1} for the Glu102-mutant HL labeled with the 2′,3′-epoxypropyl β-glycoside of *N*-acetyllactosamine (E102-HL/GAL-NAG-EPO complex)]. The cross-rotation search was performed using Patterson vectors in the range of 15.0−4.0 Å. In both cases, single dominant peaks (8.4 σ and 7.5 σ above the mean value, respectively) were obtained. The translation search was performed using 15.0−4.0 Å data. The rigid-body refinement for the solution with the highest correlation (10.5 σ and 11.0 σ above the mean value) gave *R*-values of 0.375 (8.0−2.23 Å data) and 0.380 (8.0−1.96 Å data) for the L63-HL/NAG-NAG-EPO complex and the E102-HL/GAL-NAG-EPO complex, respectively.

These models were further refined using a slow-cooling protocol in X-PLOR (initial temperature, 2000 K), which yielded an *R*-factor of 0.234 and 0.256, respectively. At this stage, individual restrained *B*-factors of the protein atoms were refined. During the final stage, 10% of the observed data was set aside for cross-validation analysis. Water molecules which could form at least one hydrogen bond with a protein atom or an already existing water molecule were included only if the final *B*-factor showed a reasonable value. The maximum *B*-values of accepted water molecules were 45.7 and 53.8 Å^2 for the L63-HL/NAG-NAG-EPO complex and the E102-HL/GAL-NAG-EPO complex, respectively. The coordinate error for both models was estimated to be less than 0.25 Å from Luzzati plots (*31*). All stereochemical parameters of the final model checked by PROCHECK (*32*) were either within or better than the average value ranges obtained from good quality models. Some data collection statistics and refinement parameters are summarized in Table 1. All graphical drawings of three-dimensional structures were produced using MOLSCRIPT (*33*) and TURBO-FRODO (*34*, *35*). The coordinates and structure factors have been deposited by the Protein Data Bank at the Research Collaboratory for Structural Bioinformatics (PDB codes: 1D6P for L63-HL/NAG-NAG-EPO complex and 1D6Q for E102-HL/GAL-NAG-EPO complex).

Table 1: Data Collection Statistics and Refinement Parameters

	L63-HL/NAG-NAG-EPO	E102-HL/GAL-NAG-EPO
crystal size (mm)	0.15 × 0.15 × 0.1	0.25 × 0.25 × 0.1
space group	$P2_12_12_1$	$P2_12_12_1$
cell dimension		
a (Å)	58.20	56.79
b (Å)	60.78	61.24
c (Å)	32.73	33.02
resolution range (Å)	22.27−2.23	22.45−1.96
no. of unique reflections	11298	10873
redundancy	3.4	3.0
R_{merge} (%)[a]	10.0 (22.27−2.23 Å)	14.9 (22.45−1.96 Å)
resolution range used for refinement (Å)	8.0−2.23	8.0−1.96
R_{merge} (%) in last shell	29.3 (2.32−2.23 Å)	27.6 (2.02−1.96 Å)
completeness of data (%)	98.3	94.0
no. of reflections used ($\|F\| > 2\sigma(F)$)	3865	6239
no. of protein atoms	1025	1030
no. of ligand atoms	33	30
no. of solvent molecules	43	62
final *R*-factor (%)	18.1	18.4
final free *R*-factor (%)	21.6	24.8
rms deviations		
bond length (Å)	0.011	0.011
bond angle (deg)	1.87	1.59
dihedral angle (deg)	25.3	24.9
improper angle (deg)	1.46	1.43
average *B*-factor (Å^2)		
protein backbone	12.9	14.5
protein side chain	15.0	19.8
protein all	14.0	17.4
solvent molecules	23.1	31.1
residues in most favored regions of phi−psi plot (%)[b]	93.0	88.7

[a] $R_{merge} = \sum_{hkl}|I_i - \langle I\rangle|/\langle I\rangle$, where I_i and $\langle I\rangle$ are the *i*th intensity and the average intensity of *i* observations, respectively. [b] Non-Gly and non-Pro residues.

RESULTS

Selection of the Mutation. Two affinity-labeled mutant HLs were selected for the X-ray structural analyses in this study. The main purpose of the first mutation was to clarify the importance of the stacking constraint by the Tyr63 residue in determining the precise position of the *N*-acetylglucosamine residue at subsite B of HL. The replacement of Tyr63 in HL to Leu or Ala has reduced catalytic action against *M. luteus* cells and *p*-nitrophenyl chitopentaoside by decreasing the affinity toward substrates (*36*, *37*). In the present study, the Tyr63→Leu mutation was chosen to avoid a large change in the hydrophobicity of the side chain.

The second mutation was selected to examine the importance of a hydrogen bond, which might play a critical role in substrate recognition of wild-type HL. In the last paper, we reported the dual affinity labeling of HL with 2′,3′-epoxypropyl β-glycoside of *N*-acetyllactosamine (GAL-NAG-EPO) as the first example of the multiple attachment of a carbohydrate ligand to the substrate-binding site of HL (*25*). The dual labeling was virtually not observed in the reaction of wild-type HL with the corresponding derivative of *N*,*N*′-diacetylchitobiose (NAG-NAG-EPO). In the WT-HL/GAL-NAG-EPO complex, atom OD1 of Asp102 hydrogen-bonded with the 4-OH group of the galactose residue at subsite B (GAL131). In contrast, in the WT-HL/NAG-NAG-EPO complex, atom OD1 of Asp102 hydrogen-bonded with the 6-OH group of the *N*-acetylglucosamine residue at subsite B (NAG131). The alteration in hydrogen bonding putatively caused the difference in the conformation of bound disaccharides (*23*). This difference explained the significant amounts of doubly-labeled wild-type HL solely with GAL-NAG-EPO (*25*).

Table 2: Kinetic Parameters of the 102nd Residue Mutant against *M. luteus* Cells

enzyme	$K_{M,app}$ (μg/mL)	V_{max} (ΔA_{650} min^{-1} μg^{-1})	$V_{max}/K_{M,app}$
wild type	67	0.28	4.2×10^{-3}
Asp102→Asn	76	0.24	3.2×10^{-3}
Asp102→Glu	260	0.43	1.7×10^{-3}

We first analyzed the lytic activity of two mutants of Asp102 against *M. luteus* as a cellular substrate. As shown in Table 2, the replacement of Asp102 with Glu, which lengthened the side chain by one methylene group, caused a large decrease in substrate affinity as compared with the replacement of Asp102 with Asn, which altered the carboxylate group to the carboxamide group. Nevertheless, a trial examination suggested the dual labeling of Glu102-mutant HL with GAL-NAG-EPO to an extent comparable to that of wild-type HL. This unexpected result prompted us to analyze the detailed three-dimensional structure of the E102-HL/GAL-NAG-EPO complex.

Affinity Labeling of Mutant Human Lysozymes. The reaction of mutant HLs with the labeling reagents apparently proceeded in the same way as observed with wild-type HL. Judging from the lytic activity against *M. luteus*, the Leu63-mutant HL and Glu102-mutant HL exhibited 5% and 1%, respectively, of residual activity. Figure 1 shows the cation-exchange HPLC elution profile of the reaction mixture of mutant HLs with each affinity labeling reagent at this stage. The elution profiles in combination with MALDI-TOF/MS analysis indicated that single labeling was dominant in both cases (Figure la,b). However, a significant amount of the doubly labeled protein, comparable to that of wild-type HL

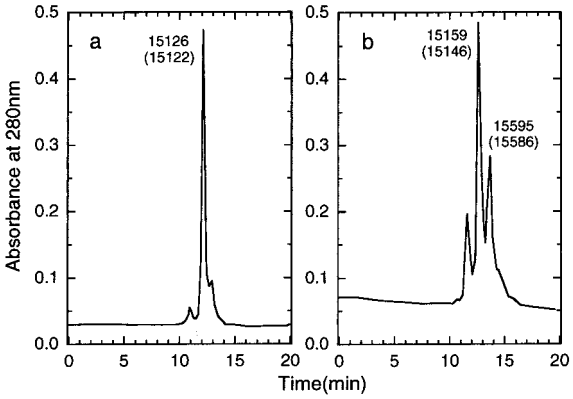

FIGURE 1: Cation-exchange HPLC profiles of the reaction mixture of mutant HL with the affinity labeling reagent. (a) Leu63-mutant HL with NAG-NAG-EPO; (b) Glu102-mutant HL with GAL-NAG-EPO. The linear gradient consisted of 0−50% NaCl in 25 mM sodium phosphate buffer (pH 7.0) for 20 min. The numerical values inside the charts indicate the measured molecular weight of the labeled peak fractions. Theoretical value in parentheses.

(*25*), was also generated in the labeling reaction of Glu102-mutant HL with GAL-NAG-EPO (Figure lb).

Structures of the L63-HL/NAG-NAG-EPO Complex and the E102-HL/GAL-NAG-EPO Complex. Each singly-labeled mutant HL was purified and crystallized for analysis by X-ray diffraction methods. Figure 2 shows the omit ($F_o - F_c$) electron density maps of the bound ligand. The well-shaped electron densities in the maps clearly delineated the conformation of the ligands. The stereochemical parameters of each disaccharide were compared with the values in the corresponding wild-type HL/ligand complex and summarized in Table 3. The stereochemical parameters of the NAG131−NAG132 linkage in the L63-HL/NAG-NAG-EPO complex were changed slightly from the corresponding values in the WT-HL/NAG-NAG-EPO complex, though these deviations remained within approximately 10%. The parameters of the GAL131−NAG132 linkage in the E102-HL/GAL-NAG-EPO complex did not show any substantial differences from the values in the WT-HL/GAL-NAG-EPO complex.

Table 4 summarizes the positional rms deviations of pyranose rings in each labeled mutant HL as compared to the labeled wild-type HL. The overall rms deviations of the L63-HL/NAG-NAG-EPO complex versus the WT-HL/NAG-NAG-EPO complex and those of the E102-HL/GAL-NAG-EPO complex versus the WT-HL/GAL-NAG-EPO complex were 0.24 Å and 0.28 Å, respectively, after rms fitting using all α-carbon atoms in the protein molecule. The deviations of the pyranose rings after the rms fitting using all ligand atoms were always less than the overall rms deviations. However, the deviation concerning NAG131 after the rms fitting using all α-carbon atoms in the protein molecule (0.80 Å) was remarkably larger than the overall rms deviation (0.24 Å) as displayed in Table 4. The data suggested that the conformations of both disaccharides were conserved, and that only the NAG131 residue in the L63-HL/NAG-NAG-EPO complex showed substantial movement in the binding cleft relative to the corresponding residue of the wild-type complex.

The ($2F_o - F_c$) electron density maps revealed the structure of each mutant HL/ligand complex (Figure 3). Both disaccharide moieties of the labeling reagent occupy subsites B and C in the productive binding mode as in the corresponding wild-type HL/ligand complex. However, the superposition of models revealed that the NAG131 residue in the L63-HL/NAG-NAG-EPO complex moved away from the side chain of Leu63 relative to the positions of NAG131 and the side chain of Tyr63 in the WT-HL/NAG-NAG-EPO complex (Figure 4a). On the other hand, the position of the *N*-acetyllactosamine moiety was virtually unaffected by the mutation of Asp102 to Glu (Figure 4b). Interaction between GAL131 and Glu102 was maintained by the movement of backbone residues 102−104 (Figure 4b).

Figure 5 shows a schematic representation of the possible hydrogen-bonding interactions (less than 3.3 Å) responsible for the recognition of the disaccharide by the protein. The number of hydrogen bonds directed toward the *N*,*N*′-diacetylchitobiose moiety including one mediated by the water molecule was decreased from 17 to 4 by the replacement of Tyr63 with Leu (Figure 5a). In contrast, the mutation of Asp102 to Glu did not greatly affect the hydrogen-bonding interaction with the *N*-acetyllactosamine moiety. In this substitution, the hydrogen bond between the side chain carboxylate group of residue 102 and the 4-OH group of the GAL131 residue was retained. Only the relocation of 2 out of 11 hydrogen bonds occurred without a net loss or gain in the total number of hydrogen bonds (Figure 5b).

DISCUSSION

The synergy in hydrogen bond and van der Waals interactions, including a stacking interaction involving an aromatic residue, occurs frequently in protein−carbohydrate complex formation responsible for various biological functions (*38*−*41*). In previous studies, we revealed the similarities and differences in the recognition of *N*-acetylglucosamine (GlcNAc), galactose (Gal), and mannose (Man) residues in subsite B of HL (*23*, *24*). As for GlcNAc and Man, each of which has an equatorial 4-OH group, the phenol side-chain group in Tyr63 of HL stacked with an apolar face of the carbohydrate residue. Additionally, the Asp102-OD1 atom in HL was involved in favorable hydrogen bonding with the 6-OH group of the carbohydrate residue (bond length: 2.6 Å in both cases). On the other hand, in the recognition of Gal, the Asp102-OD1 atom in the WT-HL/GAL-NAG-EPO complex hydrogen-bonded to the axial 4-OH group of Gal (bond length; 2.7 Å) at the expense of a reduced stacking interaction.

The importance of an aromatic residue at subsite B in the catalytic action of *c*-type lysozyme has been demonstrated by mutagenesis studies (*37*, *42*). However, the effect of losing the stacking constraint involving an aromatic side-chain group on the conformation of a carbohydrate moiety at subsite B in the productive binding mode has not yet been clarified. Recently, researchers have pointed out that a weak attractive force called the CH−π interaction may play an important role in many biological recognition processes, including the recognition of carbohydrates by proteins (*43*). The present study has examined the contribution of such interactions in determining the precise position of a carbohydrate residue at subsite B of HL.

Table 5 summarizes the possible CH−π interactions in subsite B of the wild-type and mutant HLs deduced from the refined X-ray structures. Owing to the lack of a π-electron system in the side-chain group of Leu63, the L63-HL/NAG-

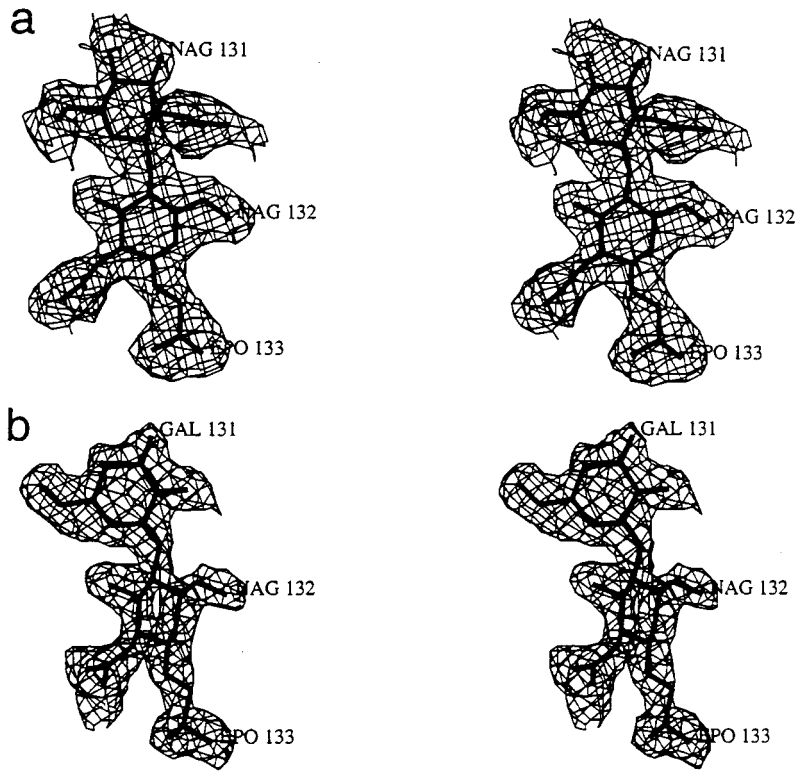

FIGURE 2: Stereoview of the ($F_o - F_c$) omit electron density map for the ligand part together with the refined model. (a) L63-HL/NAG-NAG-EPO complex; (b) E102-HL/GAL-NAG-EPO complex. The maps are contoured at 1.2 σ and 2.0 σ, respectively.

Table 3: Stereochemical Parameters of the Disaccharide Part[a]

glycoside linkage (molecule)	ϕ (deg)	ψ (deg)	ψ_H (deg)	O5−O3′ (Å)
NAG131-NAG132 (L63-HL/NAG-NAG-EPO)	−79	−130	31	2.8
NAG131-NAG132 (WT-HL/NAG-NAG-EPO)[b]	−84	−120	35	3.0
GAL131-NAG132 (E102-HL/GAL-NAG-EPO)	−70	−116	55	3.0
GAL131-NAG132 (WT-HL/GAL-NAG-EPO)[b]	−69	−119	53	3.0

[a] Values of ϕ and ψ are the torsion angles about C1−O1(O4′) and O1(O4′)−C4 defined by O5−C1−O1(O4′)−C4′ and C1−O1(O4′)−C4′−C5′, respectively. The value of ψ_H is the helical twist parameter defined as the average of the pseudorotation angles ψ_1 = O5−C1−C4′−C3′ and ψ_2 = C2−C1−C4′−C5′ (*44*). [b] Values are those in the structure determined by Muraki et al. (*23*).

Table 4: Positional Deviation of the Pyranose Ring[a]

		131st residue		132nd residue	
source molecule	target molecule	rms(P)[b]	rms(L)[c]	rms(P)[b]	rms(L)[c]
L63-HL/NAG-NAG-EPO	WT-HL/NAG-NAG-EPO	0.80	0.13	0.26	0.18
E102-HL/GAL-NAG-EPO	WT-HL/GAL-NAG-EPO	0.12	0.13	0.11	0.05

[a] Units in angstroms. The positional rms deviations of pyranose ring atoms (C1, C2, C3, C4, C5, and O5) were calculated. [b] Values are after rms fitting using all α-carbon atoms in the protein molecule. [c] Values are after rms fitting using all ligand atoms.

NAG-EPO complex lost four possible CH−π interactions compared to the WT-HL/NAG-NAG-EPO complex. In the replacement of Tyr63 with Leu, the decrease in apolar interactions altered the position of NAG131 in the L63-HL/NAG-NAG-EPO complex from its original position in the corresponding WT−HL complex, resulting in a significant loss of polar hydrogen-bonding interactions as shown in Figure 5a. Specifically, 2 direct hydrogen bonds and 11 water-mediated hydrogen bonds were lost, which should account for the decrease of binding energy in the transition state in the hydrolysis of *p*-nitrophenyl chitopentaoside by the mutation (2.6 ± 0.6 kcal mol^{-1}) (*37*). Furthermore, the Tyr63 residue in the WT-HL/NAG-NAG-EPO complex was virtually replaced by Leu using the "replace res" function of TURBO-FRODO while saving the previous positions of α- and β-carbons (*34*, *35*) for the purpose of exploring the possibility of collision between the imaginary Leu63 residue and the actual NAG131 residue. The closest distance between non-hydrogen atoms in the system was 2.5 Å after conducting the free rotation search around either the Cα−Cβ bond or the Cβ−Cγ bond. The computer-modeling experiment nearly ruled out the possibility that the positional change of the NAG131 residue, which was accompanied by the replacement of Tyr63 to Leu, could be caused by simple steric hindrance. Consequently, we propose that the CH−π interactions between Tyr63 and NAG131 function as a major determinant of the precise positioning of GlcNAc required for the strong recognition at subsite B of HL. The basis for this assumption stems from comparison of the actual complex structures in the productive binding mode.

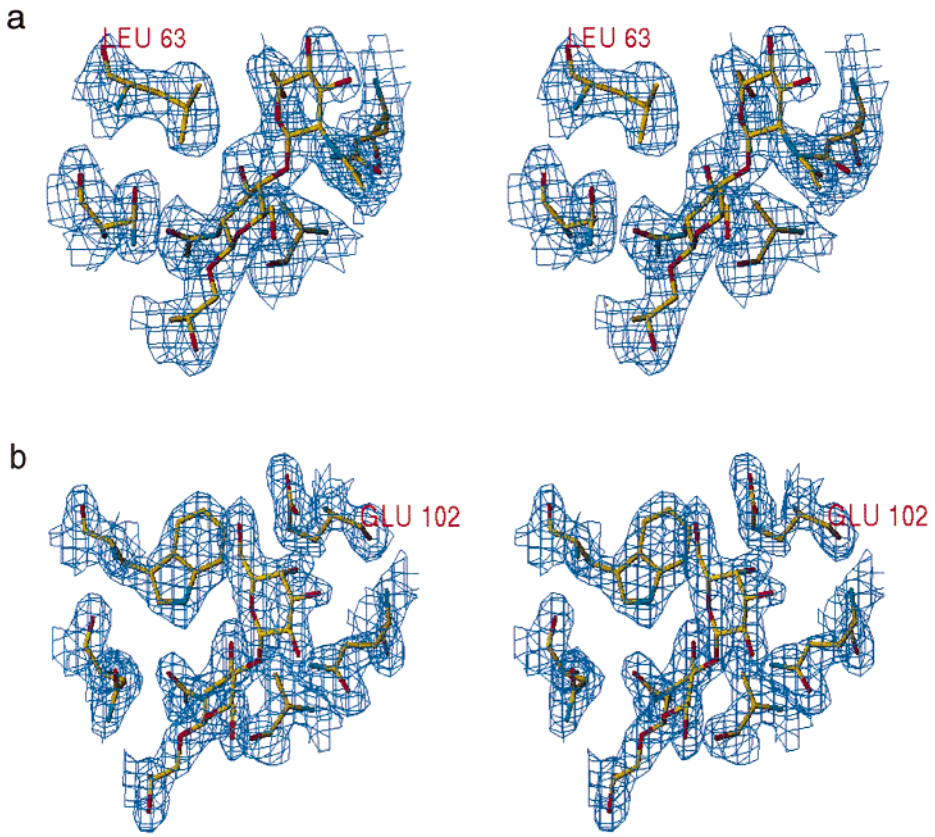

FIGURE 3: Stereoview of the ($2F_o - F_c$) electron density map for the ligand-binding structure together with the refined model. (a) L63-HL/NAG-NAG-EPO complex; (b) E102-HL/GAL-NAG-EPO complex. The maps are contoured at 0.8 σ and 1.0 σ, respectively.

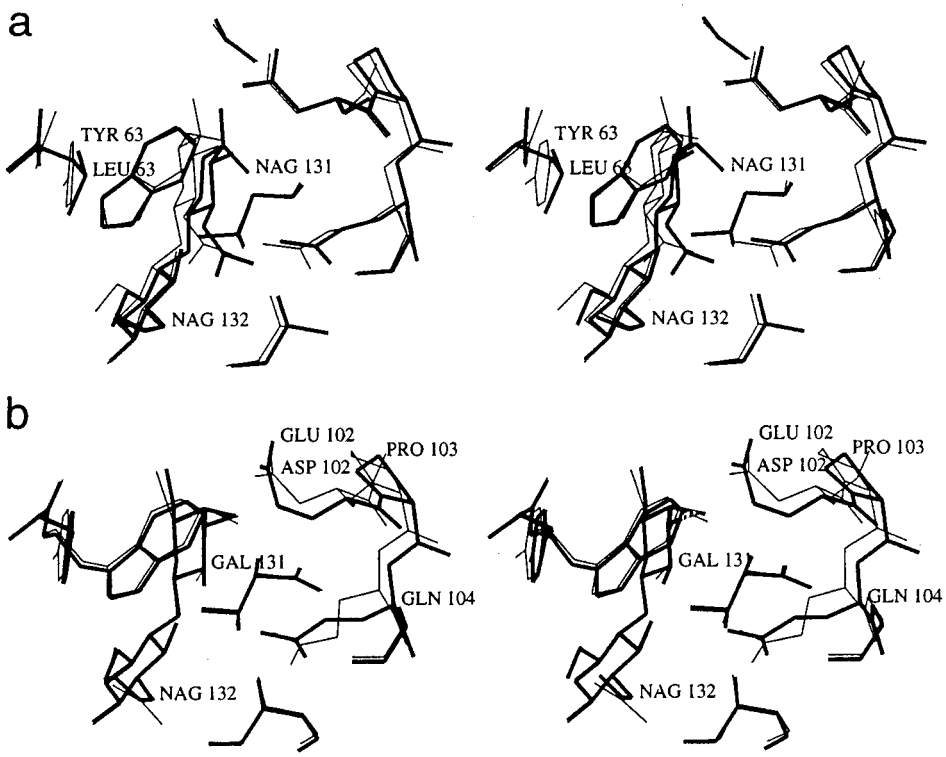

FIGURE 4: Stereoview of the superimposed binding structures of the disaccharide part. (a) L63-HL/NAG-NAG-EPO complex (thick line) and WT-HL/NAG-NAG-EPO complex (thin line); (b) E102-HL/GAL-NAG-EPO complex (thick line) and WT-HL/GAL-NAG-EPO complex (thin line).

The attachment of the affinity label to wild-type HL was accompanied by the movement of residues 102−104 (*23*). A similar conformational change was found in the loop region centered around Asp101 in hen egg-white lysozyme (*18*). The E102-HL/GAL-NAG-EPO complex acquired one additional CH−π interaction compared to the WT-HL/GAL-

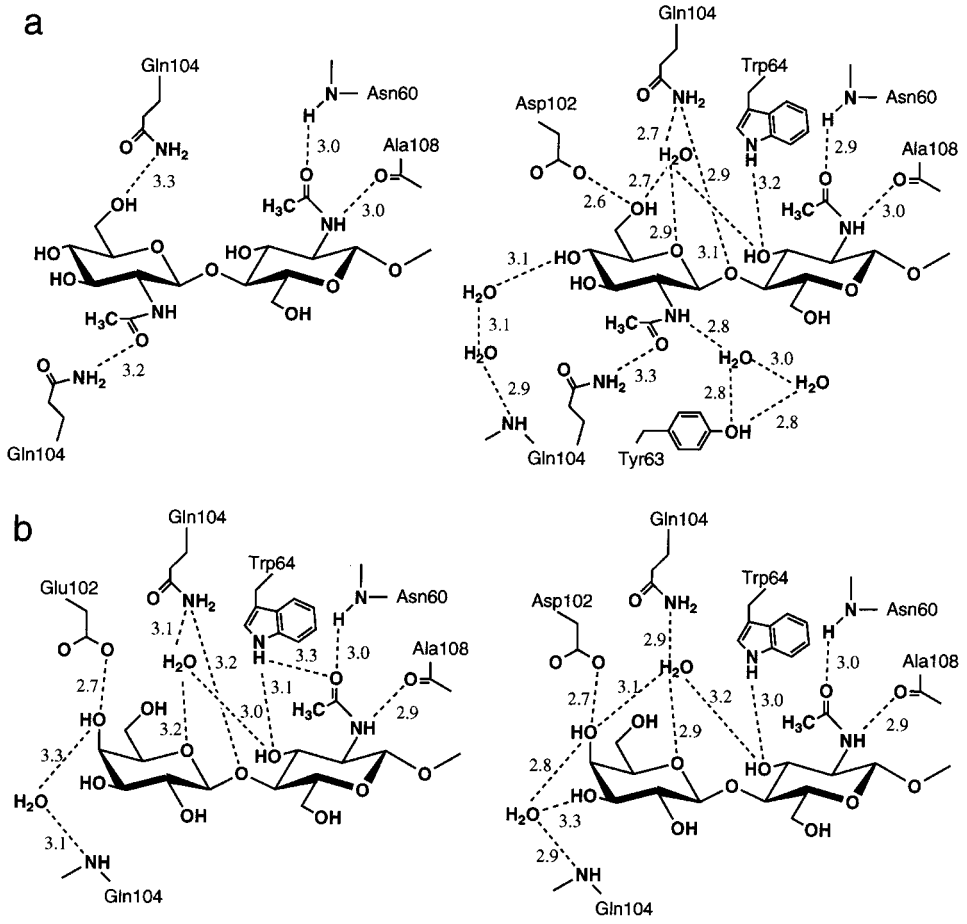

FIGURE 5: Possible hydrogen-bonding interactions between the protein part and the disaccharide part. (a) L63-HL/NAG-NAG-EPO complex (left), WT-HL/NAG-NAG-EPO complex (right); (b) E102-HL/GAL-NAG-EPO complex (left), WT-HL/GAL-NAG-EPO complex (right).

Table 5: Possible CH−π Interactions in Subsite B[a]

molecule	carbohydrate atom	protein atom	distance (Å)
WT-HL/NAG-NAG-EPO	NAG131-H1	Tyr63-CE1	2.9
	NAG131-H1	Tyr63-CZ	3.0
	NAG131-H5	Tyr63-CE2	3.0
	NAG131-H5	Tyr63-CD2	2.8
L63-HL/NAG-NAG-EPO[b]	none	none	
WT-HL/GAL-NAG-EPO	GAL131-H5	Tyr63-CD2	3.2
	GAL131-H5	Tyr63-CE2	3.2
E 102-HL/GAL-NAG-EPO	GAL131-H1	Tyr63-CZ	3.2
	GAL131-H5	Tyr63-CD2	3.0
	GAL131-H5	Tyr63-CE2	2.9

[a] Hydrogen atoms in the 131st carbohydrate residue were generated by using "hbuild protocol" in X-PLOR ver. 3.1 (*30*). Only interactions less than 3.2 Å are listed. [b] No π-electron system in Leu63. The closest distance between the hydrogen atom in NAG 131 and the carbon atom in Leu63 is 3.5 Å (NAG131-H5 to Leu63-CD1).

NAG-EPO complex (Table 5), which may contribute to the positional stability of the GAL131 residue (Figure 4b). In the replacement of Asp102 with Glu, the flexible loop region adjusted its conformation so that the hydrogen-bonding interaction between the carboxylate side-chain group of residue 102 and the 4-OH group of GAL131 residue was maintained (Figures 4b and 5b). Owing to this movement (0.63 Å as evaluated by the positional rms deviation of the main-chain atoms in the region of 102nd to 104th residues), the positions of the atoms involved in the direct hydrogen bond with the second *N*-acetyllactosamine moiety in the doubly-labeled wild-type HL (*25*) were also conserved. The rms deviation of the atoms (GAL131-O2, GAL131-O3, NAG132-O4, EPO133-O2, Gln104-OE1 and NE2, Arg107-O, Ala108-O, Trp109-N) (0.31 Å) was comparable to the rms deviation of the overall protein molecule (0.28 Å). Therefore, in conjunction with the observation of the reaction product doubly-labeled by GAL-NAG-EPO (Figure 1b), the first ligand-assisted recognition of the second *N*-acetyllactosamine moiety might have occurred here as well with the Glu102-mutant HL.

The loss of conformational flexibility of oligosaccharides upon binding to proteins has been pointed out by Imberty et al. (*16*). It was observed that both disaccharides in this study did not change their conformation from the original ligand-binding structure in the WT-HL/disaccharide complex under the condition in which either an apolar or a polar interaction was anticipated to be disturbed. The rigidness of the β1,4-linkage with the linked O4 atom in the equatorial position, such as Man-β1,4-GlcNAc, GlcNAc-β1,4-GlcNAc, Gal-β1,4-GlcNAc, and Gal-β1,4-Glc, was also predicted theoretically using potential energy calculations (*16*). The stability of the β1,4-linked disaccharide conformation under perturbing conditions may be useful for the rational design of the carbohydrate-binding proteins with the recognition specificity toward the above sequences. Finally, the methodology and findings in this study may be applicable to other protein−carbohydrate systems, which play vital roles in a number of biologically important phenomena.

ACKNOWLEDGMENT

We acknowledge Mr. Hiroshi Hashimoto (Hokkaido System Science Co., Ltd.) for his assistance in MALDI-TOF/MS analyses.

REFERENCES

1. Quiocho, F. A. (1986) *Annu. Rev. Biochem. 55*, 287−315.
2. Lee, Y. C., and Lee, R. T. (1996) *Acc. Chem. Res. 28*, 321−327.
3. Jollès, P., and Jollès, J. (1984) *Mol. Cell. Biochem. 63*, 165−189.
4. Imoto, T. (1996) in *EXS* (Jollès, P., Ed.) Vol. 75, pp 163−181, Birkhauser Verlag, Basel.
5. Lee-Huang, S., Huang, P. L., Sun, Y., Huang, P. L., Kung, H.-F., Blithe, D. L., and Chen, H.-C. (1999) *Proc. Natl. Acad. Sci. U.S.A. 96*, 2678−2681.
6. Elgavish, S., and Shaanan, B. (1997) *Trends Biochem. Sci. 22*, 462−467.
7. Vyas, N. K. (1991) *Curr. Opin. Struct. Biol. 1*, 732−740.
8. Weis, W. I., and Drickamer, K. (1996) *Annu. Rev. Biochem. 65*, 441−473.
9. Quiocho, F. A., Spurlino, J. C., and Rodseth, L. E. (1997) *Structure 5*, 997−1015.
10. Strynadka, N. C. J., and James, M. N. G. (1991) *J. Mol. Biol. 220*, 401−424.
11. Cheetham, J. C., Artymiuk, P. J., and Phillips, D. C. (1992) *J. Mol. Biol. 224*, 613−628.
12. Hadfield, A. T., Harvey, D. J., Archer, D. B., MacKenzie, D. A., Jeenes, D. J., Radford, S. E., Lowe, G., Dobson, C. M., and Johnson, L. N. (1994) *J. Mol. Biol. 243*, 856−872.
13. Song, H., Inaka, K., Maenaka, K., and Matsushima, M. (1994) *J. Mol. Biol. 244*, 522−540.
14. Noguchi, S., Miyawaki, K., and Satow, Y. (1998) *J. Mol. Biol. 278*, 231−238.
15. Vollan, V. B., Hough, E., and Karsen, S. (1999) *Acta Crystallogr. D55*, 60−66.
16. Imberty, A., Bourne, Y., Cambillau, C., Rougé, P., and Pérez, S. (1993) *Adv. Biophys. Chem. 3*, 71−117.
17. Toone, E. J. (1994) *Curr. Opin. Struct. Biol. 4*, 719−728.
18. Maenaka, K., Matsushima, M., Kawai, G., Kidera A., Watanabe, K., Kuroki, R., and Kumagai, I. (1998) *Biochem. J. 333*, 71−76.
19. Maenaka, K., Matsushima, M., Song, H., Sunada, F., Watanabe, K., and Kumagai, I. (1995) *J. Mol. Biol. 247*, 281−293.
20. White, A., and Rose, D. R. (1997) *Curr. Opin. Struct. Biol. 7*, 645−651.
21. Withers, S. G., and Abersold, R. (1995) *Protein Sci. 4*, 361−372.
22. Thomas, E. W., McKelvy, J. F., and Sharon, N. (1969) *Nature 222*, 485−486.
23. Muraki, M., Harata, K., Sugita, N., and Sato, K.-I. (1996) *Biochemistry 35*, 13562−13567.
24. Muraki, M., Harata, K., Sugita, N., and Sato, K.-I. (1998) *Acta Crystallogr. D54*, 834−843.
25. Muraki, M., Harata, K., Sugita, N., and Sato, K.-I. (1999) *Biochemistry 38*, 540−548.
26. Muraki, M., Morikawa, M., Jigami, Y., and Tanaka, H. (1989) *Eur. J. Biochem. 179*, 573−579.
27. Muraki, M., Jigami, Y., Tanaka, H., Kishimoto, F., Agui, H., Ogino, S., and Nakasato, S. (1985) *Agric. Biol. Chem. 49*, 2829−2831.
28. Locquet, J.-P., Saint-Blancard, J., and Jollès, P. (1968) *Biochim. Biophys. Acta 167*, 150−153.
29. Thomas, E. W. (1970) *Carbohydr. Res. 13*, 225−228.
30. Brünger, A. T. (1992) *X-PLOR* ver. 3.1 Manual, pp 1−269, Yale University Press, New Haven and London.
31. Luzzati, V. (1952) *Acta Crystallogr. 5*, 802−810.
32. Laskowski, R. A., McArthur N. W., Moss, D. S., and Thornton J. M. (1993) *J. Appl. Crystallogr. 26*, 283−291.
33. Kraulis, P. (1991) *J. Appl. Crystallogr. 11*, 269−272.
34. Jones, T. A. (1978) *J. Appl. Crystallogr. 25*, 348−357.
35. Roussel, A., Fontecilla-Camps, J.-C., and Cambillau, C. (1990) *J. Mol. Graphics 8*, 86−88.
36. Muraki, M., Morikawa, M., Jigami, Y., and Tanaka, H. (1987) *Biochim. Biophys. Acta 916*, 66−75.
37. Muraki, M., Harata, K., and Jigami, Y. (1992) *Biochemistry 31*, 9212−9219.
38. Bourne, Y., Rougé, P., and Cambillau, C. (1992) *J. Biol. Chem. 267*, 197−203.
39. Vyas, M. N., Vyas, N. K., and Quiocho, F. A. (1994) *Biochemistry 33*, 4762−4768.
40. Kadziola, A., Søgaard, M., Svensson, B., and Haser, R. (1998) *J. Mol. Biol. 278*, 205−217.
41. Schmidt, A. K., Cottaz, S., Driguez, H., and Schulz, G. E. (1998) *Biochemistry 37*, 5909−5915.
42. Maenaka, K., Kawai, G., Watanabe, K., Sunada, F., and Kumagai, I. (1994) *J. Biol. Chem. 269*, 7070−7075.
43. Nishio, M., Hirota, M., and Umezawa, Y. (1998) *CH/π interaction, Evidence, Nature, and Consequences*, pp 175−202, Wiely-VCH, New York.
44. Mo, F., and Jensen, L. H. (1978) *Acta Crystallogr. B34*, 1562−1569.

BI991402Q